

## Selection of Spiral Waves in Excitable Media with a Phase Wave at the Wave Back

V. S. Zykov, N. Oikawa, and E. Bodenschatz

Max Planck Institute for Dynamics and Self-Organization, D-37077 Goettingen, Germany

(Received 21 June 2011; published 14 December 2011)

Universal relationships between the medium excitability and the angular velocity and the core radius of rigidly rotating spiral waves in excitable media are derived for situations where the wave front is a trigger wave and the wave back is a phase wave. Two universal limits restricting the region of existence of spiral waves in the parameter space are demonstrated. The predictions of the free-boundary approach are in good quantitative agreement with results from numerical reaction-diffusion simulations performed on the Kessler-Levine model.

DOI: 10.1103/PhysRevLett.107.254101

PACS numbers: 05.45.-a, 05.65.+b, 47.54.-r, 82.40.Ck

Rotating spiral waves in excitable media determine the spatiotemporal dynamics in many physical, chemical and biological systems. They are found, for example, in the tachycardia and fibrillation of the heart, in catalytic surface reactions, in concentration waves of the Belousov-Zhabotinsky reaction, and in dynamics of cell aggregation [1–3]. The angular velocity and the spiral wave shape are uniquely determined by the parameters of the local kinetics and the diffusive coupling within the medium. An understanding of this selection principle can be applied, for instance, for screening of antiarrhythmic drugs and development of innovative diagnostic and therapeutic strategies.

An excitation wave is induced by a diffusive flux at a wave front triggering the medium from the resting state to an excited one. Under certain conditions the inverse transition toward the resting state is also triggered by a diffusive flux at the wave back [4]. Such a wave is called a trigger-trigger (TT) wave. In many systems, no TT waves are observed but instead trigger-phase (TP) waves, where the medium returns to the resting state when the intrinsic, local kinetics reaches a specific end point and the diffusive flux is not so crucial. Both types of waves are equally important for applications.

For TT waves a free-boundary approach has been successfully applied to analyze formation of spiral waves and other wave patterns in excitable media [5–9]. This approach is based on an eikonal equation for the normal velocity of the excited domain boundary

$$c_n = c_p - Dk, \quad (1)$$

where  $c_p$  is the velocity of a plane boundary,  $k$  is the boundary curvature and  $D$  is the diffusion coefficient.

For TP waves the normal velocity of the wave back is not determined by Eq. (1) and till now spiral wave selection in excitable media with TP waves remains unsolved.

In this Letter we derive universal relationships between the medium excitability and the selected angular velocity and the core radius of rigidly rotating spiral waves in excitable media supporting TP waves.

Our analysis is based on a modified free-boundary approach, which can be applied for excitable medium models of different forms. As an example the Kessler-Levine (KL) model is used, which was originally aimed to simulate spiral dynamics during the cell aggregation in *Dictyostelium discoideum* [10,11]. The aggregation is controlled by chemical signaling molecules cAMP diffusing through the intercellular space. The KL model describes the spatiotemporal variations of the cAMP concentration,  $u$ , by the two-component reaction-diffusion system

$$\frac{\partial u}{\partial t} = D\nabla^2 u + F(u, v), \quad (2)$$

$$\frac{\partial v}{\partial t} = G(u, v), \quad (3)$$

with a specific kinetic term

$$F(u, v) = -\chi u + AH(u - a)[1 - H(v - \tau)], \quad (4)$$

where  $H$  is the Heaviside function. This kinetic function assumes that, when the cAMP concentration near a cell exceeds a threshold  $a$ , the cell becomes excited and emits a fixed amount of the cAMP during a time interval  $\tau$  with a constant intensity  $A$ . The coefficient  $\chi$  specifies the degradation rate of cAMP within the extracellular space.

The value  $v$  in Eq. (4) has a physical meaning of a time counted from the last excitation. Hence,  $v$  is equal to zero in the resting state and starts to grow at the unit rate just after an excitation. At the instant when  $v$  reaches the relative refractory time,  $\tau_{rr}$ , its value has to be reset to zero. In numerical computations the growth of  $v$  can be formally described by Eq. (3) with

$$G(u, v) = H(v) \quad (5)$$

and  $v$  has to be set to a small positive value  $v_{\min} \ll \tau$  when  $u = a$  and  $du/dt > 0$  and reset to zero when it reaches  $\tau_{rr}$ .

During the time interval between the absolute refractory period,  $\tau_{ar}$ , and the relative refractory period,  $\tau_{rr}$ , the excitation threshold  $a$ , which determines the planar velocity  $c_p$ , is specified by

$$a = a_{\max} - \eta(v - \tau_{\text{ar}})/v, \quad (6)$$

where  $\eta = (a_{\max} - a_{\min})\tau_{\text{rr}}/(\tau_{\text{rr}} - \tau_{\text{ar}})$ . Here  $a_{\max}$  and  $a_{\min}$  specify the threshold value during the absolute refractory period and in the resting state, respectively.

In one-dimensional simulations a propagating wave consists of a trigger front and a wave back following the front after the fixed time interval  $\tau$ . Obviously, it is a TP wave with the back velocity predetermined by the front motion. It is shown below, that this property strongly affect dynamics of two-dimensional spiral waves.

The main assumption of the free-boundary approach is that the front and the back of a propagating wave are thin in comparison to the wave plateau and, hence, the spiral wave dynamics is completely determined by the motion of the excited domain boundary, e.g., the curve  $u(x, y, t) = a$ . The normal velocity of the boundary is positive at the wave front, is negative at the wave back and vanishes at their common point  $q$ , so-called phase change point [12]. In the case of a rigidly rotating spiral, the normal boundary velocity  $c_n$ , the tangential one  $c_\tau$  and the curvature  $k$  obey pure kinematic equations [9]

$$\frac{dc_n}{ds} = \omega + kc_\tau, \quad (7)$$

$$\frac{dc_\tau}{ds} = -kc_n, \quad (8)$$

where  $s$  is the arc length counted from the point  $q$  and  $\omega$  is the angular velocity.

If the relative refractoriness is shorter than the rotation period, the front velocity of a spiral wave induced in the KL model is simply proportional to the boundary curvature according to Eq. (1), where  $c_p = c_p(a_{\min}) = \text{const}$  in this case due to Eq. (6). Then the spiral wave front is specified by a solution of the system (1), (7), and (8) starting at the phase change point with the initial conditions

$$c_n(0) = 0, \quad c_\tau(0) = c_t \quad (9)$$

and approaching asymptotically for  $s \rightarrow \infty$  the values

$$c_n(\infty) = c_p, \quad c_\tau(\infty) = -\infty. \quad (10)$$

For a given value of the tangential velocity of the phase change point  $0 < c_t < c_p$  Eqs. (1) and (7)–(10) determine a nonlinear boundary value problem. The solution of this problem specifies the single possible value of the angular velocity  $\omega$  and the corresponding functions  $c_n(s)$ ,  $c_\tau(s)$ , and  $k(s)$  [9]. The last function determines the selected shape of the spiral wave front in Cartesian coordinates by the following system of equations:

$$d\Theta/ds = -k, \quad dx/ds = \sin(\Theta), \quad dy/ds = \cos(\Theta), \quad (11)$$

where angle  $\Theta(s)$  specifies the normal direction.

As an example, the spiral front obtained numerically for  $c_p = 2$ ,  $c_t = 0.8$ ,  $D = 1$  and for the selected value  $\omega = 0.552$  is shown in Fig. 1 (thick solid). The spiral core radius is naturally determined as  $r_q = c_t/\omega$ .

It is important to stress, that the eikonal Eq. (1) remains to be valid also for the wave back within a region near the phase change point, where  $v < \tau$ . Taken this into account one can use the system (1), (7), (8), and (11) with the selected value of  $\omega$  to specify the shape of the wave back even for  $s < 0$  as shown by the thin solid in Fig. 1. On the other hand, it is clear, that far away from the phase change point the wave back should simply follow the wave front. Thus, the shape of the back should be identical to the front shape, but has to be turned around the rotation center by the angle  $\alpha = \omega\tau$ , as shown by dashed line in Fig. 1. The angle  $\alpha$  is chosen here in such a way, that a part of the wave back obeying the eikonal Eq. (1) is smoothly connected to the asymptotically established phase wave. Namely this smoothness condition determines the selected back shape and the value of  $\tau$ .

In order to generalize the obtained selection principle, it is suitable to use the values  $c_p$  and  $D$  to rescale velocities, e.g.  $C_t = c_t/c_p$ , and space variables, e.g.,  $S = c_p s/D$ ,  $X = c_p x/D$ ,  $Y = c_p y/D$ . Two important parameters appear after this rescaling. The first one is the dimensionless angular velocity

$$\Omega = \frac{\omega D}{c_p^2}. \quad (12)$$

The second one is the dimensionless parameter, which specifies the medium excitability [5,7–9]

$$B = \frac{2D}{d_u c_p^2}, \quad (13)$$

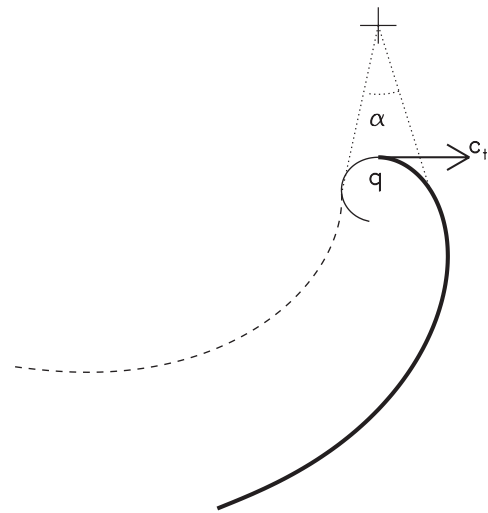


FIG. 1. The selected shape of a spiral wave rigidly rotating at  $\omega = 0.552$  obtained as a solution of the free-boundary problem (1) and (7)–(11) for  $c_p = 2.0$ ,  $c_t = 0.8$ ,  $D = 1$ , and  $\tau = 0.943$ .

where  $d_u$  is the duration of a propagating pulse. Note that  $d_u \approx \tau$ , if the excited domain boundary is thin.

The values of  $\Omega$  selected as the solution of the free-boundary problem (1) and (7)–(11) are shown in Fig. 2(a) as a function of the parameter  $B$ , which is inversely proportional to  $\tau$  due to Eq. (13). The selected value of the tangential velocity  $C_t(B)$  is also presented in Fig. 2(b).

At  $B = B_{\min}$  the spiral core radius vanishes,  $\alpha = \pi$  and the angular velocity approaches the value  $\Omega = 0.331$ , which was first found for the screw dislocation growing on a crystal surface [13]. Obviously, in this case  $\tau = \tau_m \equiv (D/c_p^2)\pi/0.331$  and  $B_{\min} = 2D/(\tau_m c_p^2) = 0.662/\pi \approx 0.211$ . This limit is practically identical to one found for the case of TT waves [9].

At  $B = B_{cp}$  the angular velocity vanishes and spiral wave is transformed to, so-called, critical finger with known analytical solution for the wave front [5]. Then  $B_{cp} = 2/\ln[(1 - \cos\Theta_{cp})/(1 + \cos\Theta_{cp})] \approx 0.977$ , where normal angle at the matching point  $\Theta_{cp} \approx 3.83$  is a solution of the equation  $\tan\Theta_{cp}/2 + 1/\tan\Theta_{cp}/2 + \pi = 0$ . Note, that for TT waves a similar transformation occurs at a quite different value  $B_c = 0.535$  [5,7–9], as shown in

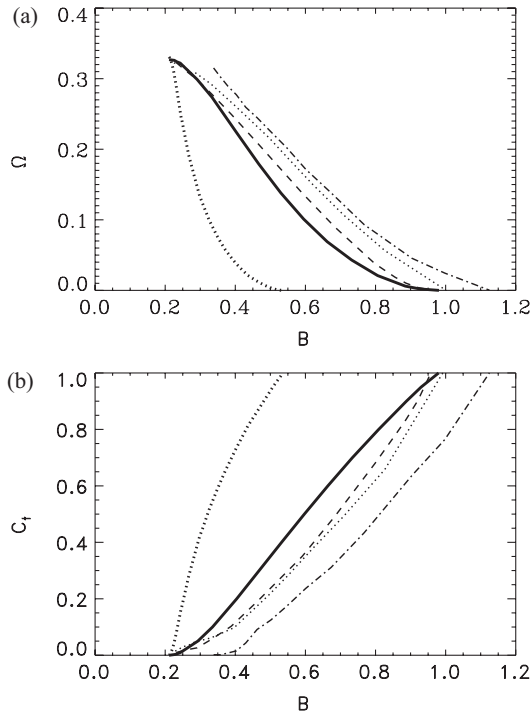


FIG. 2. The selected values of the dimensionless angular velocity  $\Omega$  (a) and the tangential velocity  $C_t$  (b) obtained from numerical solutions of the free-boundary problem (1) and (7)–(11) as functions of the dimensionless parameter  $B$  (solid lines). The results of direct integration of the KL model obtained for varying  $\tau$  with different threshold values are depicted as dotted lines for  $a' = 0.37$ , dashed lines for  $a' = 0.27$  and dashed-dotted lines for  $a' = 0.107$ . Thick dotted lines show similar dependences found for TT waves in [9].

Fig. 2. However, in a close vicinity of  $B_{cp}$  an asymptotics  $\Omega = 0.204(B_{cp} - B)^{3/2}$  is valid with the power law found earlier [14].

In order to verify the selected relationships, direct numerical integrations of the KL model have been performed. To avoid the influence of the medium refractoriness, the values of  $\tau_{ar}$  and  $\tau_{rr}$  have been chosen to be smaller than the rotation period. Moreover, if the rotation period is too short, the variable  $u$  does not have enough time to return back to the resting state, that should affect the velocity of the following front. To prevent this undesirable influence, the computations corresponding to short periods and small core radii have been performed on a helical surface instead of a plane. The explicit Euler method has been used with the space step  $\Delta x = 0.04$  and the time step  $\Delta t = 0.0002$ . For a plane the grid size was  $(500 \times 500)$  nodes. To simulate a helical surface a set of such grids centered at the origin and numbered by index  $i$  was used. The nodes of the grid  $i$ , located directly to the right of the radial line  $x = 0, y > 0$ , have been connected to the nodes laying directly to the left of this line of the grid  $i + 1$  rather than of the grid  $i$ . That enables a front of a counterrotating spiral wave to move always through the resting state passing from one grid to the next.

To systematize the simulation data, note that a dimensionless form of the KL model contains only two control parameters  $a' = a_{\min}\chi/A$  and  $\tau' = \tau\chi$ . Taking this into account, the parameters  $D = 1$ ,  $A = 3$ , and  $\chi = 8$  have been fixed, and  $\tau$  and  $a_{\min}$  have been varied.

In Fig. 2 results of our simulations are shown by three different lines corresponding to a fixed value of the parameter  $a_{\min}$  and varying parameter  $\tau$ . The angular velocity is determined from two-dimensional simulations and the propagation velocity is measured in one-dimensional computations. It can be seen, that all data obtained in the reaction-diffusion computations reproduce qualitatively the predictions of the free-boundary approach and provide rather good quantitative agreement, e.g., for  $a' = 0.27$ . Deviations increase if  $a'$  approaches 0.5 or vanishes. One reason for the observed deviations is a finite thickness of the excited domain boundary neglected by the free-boundary approach. The predicted tangential velocity of the phase change point is also in quantitative agreement with the reaction-diffusion simulations as can be seen in Fig. 2(b). Hence the core radius and the spiral shape are correctly predicted by the free-boundary approach presented here.

It is important to stress that the relations  $\Omega(B)$  and  $C_t(B)$  obtained above for short refractoriness can be used to consider the medium with an arbitrary refractoriness  $\tau_{rr}$ . For the KL model it can be done relatively easy, since for a spiral wave rigidly rotating on a plane the value of the variable  $v = T \equiv 2\pi/\omega$  is the same along the whole wave front. The plane wave velocity in Eq. (1) should be specified by the dispersion relation  $c_p(\omega)$ . The slope of the

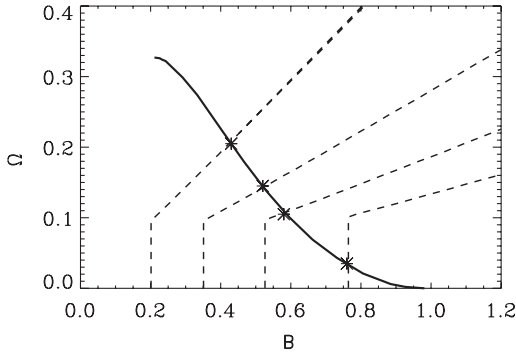


FIG. 3. Selection of the dimensionless angular velocity in the KL model with  $a_{\min} = 0.085$  and  $\tau_{\text{tr}} = 5$ . Solid line represents the relation  $\Omega(B)$  in the medium without refractoriness. Dashed lines depict the generalized dispersion relations  $\Omega_T(B)$  obtained for  $\tau = 0.75, 0.43, 0.29$ , and  $0.21$  from left to right.

eikonal equation, generally speaking, also can depend on the wave period  $T$  [15], but for the KL model it remains equal to  $D$ . Hence, only the relation  $c_p(\omega)$  should be substituted into Eqs. (12) and (13), to derive a generalized dispersion relation  $\Omega_T(B)$ , and then to solve the equation  $\Omega(B) = \Omega_T(B)$  [9]. The graphical solution of this equation is illustrated in Fig. 3.

Let denote as  $B^*$  and  $\Omega^*$  the selected values at the intersection points and the corresponding plane velocity as  $c_p^*$ . The selected tangential velocity is determined as  $C_t^* = C_t(B^*)$ . In addition  $B_0$  and  $c_0$  will specify the values of  $B$  and  $c_p$  for  $\omega = 0$ . Then the predicted rotation frequency  $\Omega_r$  and the tangential velocity  $C_{\text{tr}}$  for the given excitability  $B = B_0$  are expressed as

$$\Omega_r = (c_p^*/c_0)^2 \Omega^*, \quad C_{\text{tr}} = (c_p^*/c_0)^2 C_t^*. \quad (14)$$

The relationships obtained by use of this procedure for the KL model are shown in Fig. 4. It can be seen that for  $B > 0.6$  the refractoriness plays no role, but for smaller  $B$  refractoriness reduces the angular velocity  $\Omega$  and increases the tangential velocity  $C_t$ . These data are in a good quantitative agreement with the results of direct reaction-diffusion simulations also shown in Fig. 4.

In summary, the proposed free-boundary approach allows us to discover a selection principle for rigidly rotating spiral in a broad class of excitable media with a phase wave at the wave back. The main result of this consideration is the dimensionless angular velocity  $\Omega$  specified as a monotonically decreasing function of a single dimensionless parameter  $B$  characterizing the medium excitability.

The KL model provides probably the simplest way to reproduce TP waves in the reaction-diffusion system. By use of this model it is rather easy to separate two factors, which are equally important in the spiral wave selection, i.e., the medium excitability and the refractoriness. By exploiting this separation and by use of a helical surface instead of a plane it was possible in this Letter to study the

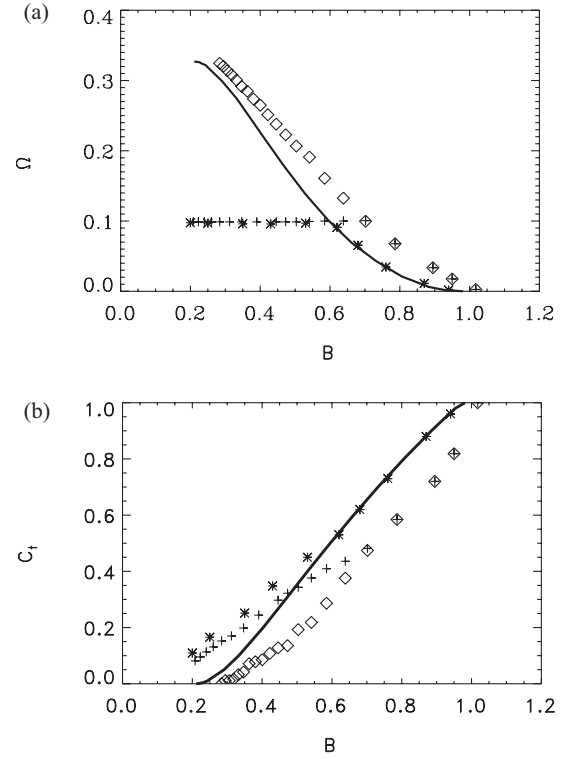


FIG. 4. The angular velocity  $\Omega_r$  (a) and spiral tip velocity  $C_{\text{tr}}$  (b) predicted in the medium with refractoriness  $\tau_{\text{tr}} = 5$  and  $\tau_{\text{ar}} = 0.4$  are shown by (\*). Functions  $\Omega(B)$  and  $C_t(B)$  obtained above with neglected refractoriness are depicted by solid lines. The data from numerical simulations with the KL model with  $a_{\min} = 0.085$  and  $a_{\max} = 0.1$  are shown by (+) for  $\tau_{\text{tr}} = 5$  and by (◇) without refractoriness.

whole parameter region  $B_{\min} < B < B_{\text{cp}}$  first neglecting refractoriness and then taking it into account.

The proposed free-boundary approach opens perspectives to analyze TP spiral waves in different kind of models with a more complicated controller dynamics. The corresponding study is important for such application as chemical or cardiac excitable media. However, it goes beyond the aim of this Letter.

- 
- [1] A. T. Winfree, *The Geometry of Biological Time* (Springer, Berlin, Heidelberg, 2000).
  - [2] A. S. Mikhailov, *Foundations of Synergetics* (Springer, Berlin, Heidelberg, 1994).
  - [3] J. D. Murray, *Mathematical Biology* (Springer, New York, 2003).
  - [4] J. J. Tyson and J. Keener, *Physica (Amsterdam)* **32D**, 327 (1988).
  - [5] A. Karma, *Phys. Rev. Lett.* **66**, 2274 (1991).
  - [6] D. Margerit and D. Barkley, *Phys. Rev. Lett.* **86**, 175 (2001).
  - [7] V. Hakim and A. Karma, *Phys. Rev. E* **60**, 5073 (1999).

- [8] V. S. Zykov and K. Showalter, *Phys. Rev. Lett.* **94**, 068302-1 (2005).
- [9] V. S. Zykov, *Physica (Amsterdam)* **238D**, 931 (2009).
- [10] D. A. Kessler and H. Levine, *Phys. Rev. E* **48**, 4801 (1993).
- [11] S. Sawai, P. A. Thomason, and E. C. Cox, *Nature (London)* **433**, 323 (2005).
- [12] F. B. Gul'ko and A. A. Petrov, *Biofizika* **17**, 261 (1972).
- [13] W. K. Burton, N. Cabrera, and E. C. Frank, *Phil. Trans. R. Soc. A* **243**, 299 (1951).
- [14] Yu. E. Elkin, V. N. Biktashev, and A. V. Holden, *Chaos Solitons Fractals* **14**, 385 (2002).
- [15] A. M. Pertsov, M. Wellner, and J. Jalife, *Phys. Rev. Lett.* **78**, 2656 (1997).